

Original Article

New Design to Provide Absolute Protection Within a Certain Period for Biodegradable Magnesium Alloys



Jian-Hua Zhu^{a,1}, Xinzhe Gao^{b,1}, Biying Shi^{b,1}, Jiawei Zou^b, Yu Ru Li^b, Ke Zeng^b, Qi Jia^b, Heng Bo Jiang^{b,*}

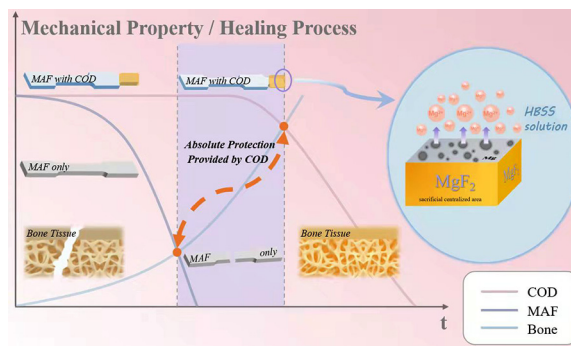
^a Department of Oral and Maxillofacial Surgery, Peking University School and Hospital of Stomatology, National Center for Stomatology, National Engineering Laboratory for Digital and Material Technology of Stomatology, Beijing Key Laboratory of Digital Stomatology, Haidian District, Beijing 100081, PR China

^b The CONVERSATIONIST club, School of Stomatology, Shandong First Medical University, Jinan, Shandong 250117, PR China

HIGHLIGHTS

- Expanding Mg corrosion test system by adding a tensile strength test.
- A design for the corrosion-oriented control of Mg by cathodic protection principle.
- The corrosion-oriented design provides mechanical property protection for Mg.

GRAPHICAL ABSTRACT



ARTICLE INFO

Article history:

Received 19 May 2022

Received in revised form 24 April 2023

Accepted 26 April 2023

Available online 3 May 2023

Keywords:

Magnesium alloy
 Corrosion resistance
 Sacrificial anode
 Microarc fluorination
 Corrosion-oriented design

ABSTRACT

Objectives: Magnesium and magnesium alloy materials have excellent potential as biodegradable bone plate implants. However, the practical application of magnesium alloys is limited by their high chemical activity and poor corrosion resistance. Here, we chose a microarc fluorination (MAF) treatment to improve corrosion resistance while enhancing aspects of magnesium alloy properties. The aim of this study was to identify the effect of fixed-point corrosion on the corrosion resistance as well as the mechanical properties of magnesium alloys and to design a new corrosion-oriented model that can provide absolute protection over a period of time.

Material and Methods: MAF treatment is used for surface modification of magnesium alloys to improve the corrosion resistance of magnesium alloys. To investigate the effect of the coating and indentation on the corrosion resistance of Mg alloy, electrochemical corrosion experiments were carried out. It is worth mentioning that in this experiment we measured and analyzed the mechanical properties of the samples, especially the tensile strength.

Results: In the innovative indentation sample test, the coated specimens showed lower tensile strength due to the occurrence of fixed-point corrosion. To avoid the loss of mechanical properties due to fixed-point corrosion, we proposed a new idea (Corrosion-oriented Design). Ultimately, the immersion experiments as well as the mechanical properties analysis concluded that the Corrosion-oriented Design samples could maintain the mechanical properties without detectable loss for a long time.

Conclusion: The Corrosion-oriented Design model can avoid the nuisance of fixed-point corrosion and control the centralized orientation of corrosion. This provides a new direction for the clinical application

* Corresponding author.

E-mail address: hengbojiang@foxmail.com (H.B. Jiang).

¹ These authors contributed equally to this work.

of magnesium alloys, which may offer a completely stable bone-healing condition in trauma treatment and avoid the drawbacks caused by the previous uncontrolled corrosion.

© 2023 AGBM. Published by Elsevier Masson SAS. All rights reserved.

1. Introduction

Magnesium (Mg) and magnesium alloy materials have a known potential for biodegradable implant applications, and studies based on the control of biodegradation are thus expanding in order to overcome the problems of undesirable dissolution processes and rates of Mg and Mg alloy materials [1]. In the last decade, researchers have reconnoitered that magnesium and its alloys have good mechanical properties, biocompatibility and osteogenesis [2–6]. Currently, there are several strategies to the defect of excessive corrosion rate of magnesium alloys, including alloy composition optimization, casting process improvement and surface modification, etc. [3,7]. It has been demonstrated that improving the protective properties of surface coatings in high chloride ion solutions such as biological fluids is a proven effective method. Among the existing surface modification techniques, microarc fluorination (MAF) is considered to be a method of operational simplicity and high efficiency during the preparation of protective fluoride coatings for Mg materials. Fluorine, in parallel with Mg, is one of the trace elements needed by the human body, while fluorine is a component of human bones and teeth [8–10]. Notably, the coating facilitates the proliferation of osteoblasts [11], which is the main reason we therefore chose the MAF coating in this study.

The fixed pitting corrosion was firstly explored as a major cause of mechanical property loss under coating conditions. This local coating disintegration at uncontrollable fixed points implies the formation and extension of cracks, which, in the presence of stress concentrations, can consequently lead to the destruction of the mechanical integrity of the implant [1,12–14]. Nowadays, more and more research about magnesium alloys is focusing on corrosion resistance while paying attention to the testing of mechanical properties [7,15]. Therefore, it is particularly critical concerning the testing and optimization of mechanical properties, especially the tensile properties, of Mg alloy materials when applied to biodegradable implants such as bone plates [16–19].

Therefore, to avoid fixed-point corrosion became the main purpose of the new design of our research. By combining the properties of Mg and Mg alloys with multidisciplinary expansion we found that as a consequence of their good electronegativity, Mg and Mg alloys are suitable in real applications as sacrificial anodes in corrosion resistant means and rarely become protected parts [20–23]. Magnesium is highly reactive and has a more negative potential than most coatings and metals. In addition, metals with a more negative potential than magnesium, such as potassium, calcium, and sodium, dissolve too quickly to meet the requirements for long-term protection. Magnesium is therefore often used as an excellent sacrificial anode material for the protection of other metals.

The innovation of our study is that it goes beyond the mindset and uses reasonable material partitioning to enable simultaneous anodic sacrifice and cathodic protection of the magnesium alloy itself for the protection of functional magnesium alloys. The optimal sacrificial anode should provide sufficient current while meeting a suitable self-dissolution rate [19,21]. In the observation of the indentation treatment group after immersion, the corrosion localization and centralization should not be neglected. Combined with the theoretical transformation of Mg alloy material when used as a sacrificial anode, we designed the Corrosion-oriented Design (COD) model (Fig. 1) with the aim of maintaining the mechanical properties of degradable Mg alloy implants, based on the control of the

overall dissolution rate of Mg alloy material, and determined its sacrificial centralized area and functional area. The design could provide absolute protection of the mechanical properties for the functional area of Mg alloys in a certain period of time. If used as bone implants, COD Mg alloys could avoid premature fracture due to the sudden change of mechanical properties in the early stage of bone healing, providing the necessary mechanical support for bone healing, and can be completely degraded at the end.

The aim of this study was to identify the effect of fixed-point corrosion on the corrosion resistance as well as the mechanical properties of magnesium alloys and to design a new corrosion-oriented model that can provide absolute protection over a period of time. The corrosion resistance and tensile strength of bare and coated magnesium alloys were measured and evaluated before and after the addition of dents. Our model design successfully utilizes the sacrificial anode principle and provides a new idea for the protection of magnesium alloys.

2. Material and methods

2.1. Materials and treatment

Commercial AZ31 Mg alloys (2.85 wt% Al; 0.75 wt% Zn; 0.62 wt% Mn; 0.025 wt% Si; 0.003 wt% Fe; 0.00045 wt% Cu; 0.00052 wt% Ni; Mg rest) were employed as the substrates. Three sample types were utilized in this experiment, including disc samples (radius of 8 mm, thickness of 2 mm), tensile samples and COD samples. The samples were divided into corrosion and sealing areas, and the COD samples were divided into functional, sealing, and sacrificial centralized areas. The sealing areas of all samples were sealed with silicone prior to the *in vitro* immersion experiments. The samples were gradually polished with silicon carbide paper in anhydrous ethanol, washed ultrasonically in anhydrous ethanol for one minute, and then blown dry for the next surface modification step. The surface modification method was applied in this experiment because the corrosion resistance of AZ31 with Mg fluoride coating obtained by microarc fluorination treatment at 200 V was proved by the previous *in vivo* and *in vitro* experiments. In 100 mL of 46% hydrofluoric acid electrolyte, the disc, tensile sample and COD were used as the anode and graphite rod as the cathode. The MAF-treated discs, tensile samples and COD samples were obtained after applying 200 V at a constant direct current (DC) voltage and a maximum current of 2A for 30 seconds. For the COD samples, a specific area, i.e., the sacrificial centralized area will be used as a corrosion orientation and one of its surfaces is not covered with a coating, called the leakage surface (Fig. 1). Bare, MAF-treated discs and tensile test plates were pressed to a depth of 0.5 mm by a Vickers hardness tester to obtain intended bare (in-Bare) and intended MAF (in-MAF), respectively.

2.2. Fixed-point corrosion analysis

To investigate the effect of MAF coating and indentation on the corrosion resistance of Mg alloy, electrochemical corrosion experiments were carried out. The electrochemical cell for the potentiodynamic polarization (PDP) tests consisted of a classical three-electrode cell with Ag/AgCl/sat-KCl (+197 mV vs. standard hydrogen electrode) as reference electrode and a working electrode with an exposed surface area of 0.9 cm². Samples were placed in

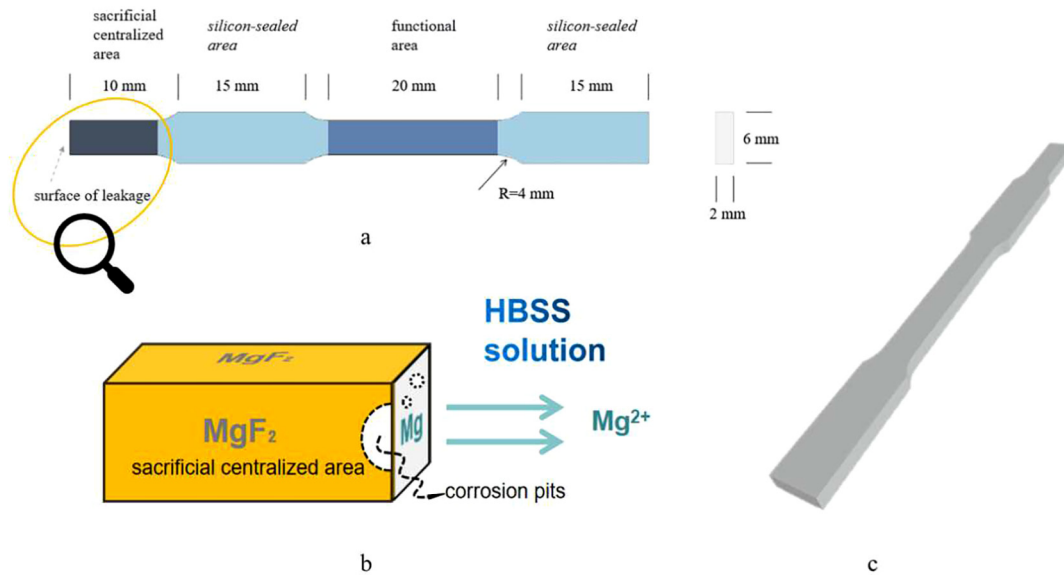


Fig. 1. Corrosion-oriented Design concept (COD) diagram and principle. **a.** Specific partition and COD model 2D image and size. Of the three partitions, the sealing area to improve the accuracy of detection, mainly in order to make the sample with a certain grip in the tensile performance testing. The functional area is used to achieve specific functions as the protected body, and is the main object to be detected in this experiment for tensile property testing. The sacrificial centralized area realizes the guiding role of fixed-point corrosion of magnesium alloy base. **b.** Corrosion guiding process. **c.** 3D image of COD model.

a sealed Teflon fixture with 37°C Hank's balanced salt solution (HBSS) was used as the electrolyte. In this experiment, samples were immersed in HBSS for one hour to perform their open circuit potential (OCP) mode. After the potential of the test sample was stabilized, it was scanned from the cathode region to the anode region at a rate of 5 mV/s over the range of -2.3 V to -0.3 V of the reference electrode value. The corrosion potentials (E_{corr}) of the four groups of Bare, in-Bare, MAF, and in-MAF were recorded. To further investigate the reason why indentation reduces the corrosion resistance of Mg alloy, short-term immersion experiments were conducted. We immersed the in-Bare and in-MAF samples vertically in HBSS and maintained the temperature at 37°C. The ratio of HBSS volume to sample area was 20 ml/cm². The surface of the indented samples was observed by optical microscopy after one week of immersion.

2.3. Tensile test after corrosion

To verify the significant effect of fixed-point corrosion on the mechanical properties, we examined the tensile strength of sample Bare, in-Bare, MAF, and in-MAF after soaking them in HBSS solution. The sealed areas of all four groups of samples were sealed with silicone prior to immersion, and the samples were immersed vertically in HBSS and maintained at 37°C for 2 weeks. Where the ratio of HBSS volume to corrosion area was 20 ml/cm² and the HBSS solution was changed once a week. After 2 weeks, 10 samples were removed from Bare, in-Bare, MAF, and in-MAF groups, respectively, and tensile tests were performed with an INSTRON tester at a constant cross-head speed of 1 mm/min after observing the sample surfaces, as well as recording the tensile curves and maximum tensile strength. In order to observe whether COD could maintain its original mechanical strength after soaking for a longer period of time, i.e., to provide stage absolute protection, we checked the tensile sample strength after soaking COD in HBSS for several weeks. Meanwhile, Bare and MAF were used as control groups. The three groups were immersed vertically in HBSS and maintained at 37°C for 4, 8, and 12 weeks. The rest of the experimental conditions were consistent with the post-corrosion tensile experiments described above. We took 10 samples from COD, Bare & MAF groups every 4 weeks, observed the sample surface and

then performed tensile tests with INSTRON testing machine at a constant cross-head speed of 1 mm/min, and recorded the tensile curves and maximum tensile strength.

2.4. Analysis

Ten samples were taken from each group and the tensile strength was expressed as mean \pm standard deviation (SD). All statistical analyses were performed using IBM SPSS Statistics Version 23.0 for Windows (IBM Corporation, Armonk, New York, USA). Statistical analysis of the results was performed using one-way analysis of variance (ANOVA) and post-processing analysis of the Tukey test. Values of $P = 0.05$ were considered significant.

3. Results

3.1. Available tests for corrosion resistance properties of indentation samples

The systematic groups of indented defect samples were exploited to obtain a fixed-point corrosion model.

3.1.1. Electrochemical experiments

Indentation sampling set was designed to demonstrate the effectiveness of the MAF coating and also to determine the conditions of fixed-point corrosion generation. In this sampling set, in addition to the original Bare and MAF sets, indentation specimens were obtained by pressing down the Vickers hardness tester to a depth of 0.50 mm, respectively. This sampling set was first subjected to electrochemical testing.

The influence of MAF coating and indentation on the corrosion resistance of magnesium alloys was carefully examined by PDP tests. A classical three-electrode cell with HBSS as electrolyte was included and the PDP experimental procedure was scanned from the cathodic to the anodic region at reference electrode values ranging from -2.3 V to -0.3 V. The corrosion potentials (E_{corr}) and corrosion current densities (I_d) were recorded for groups Bare, in-Bare, MAF and in-MAF. Fig. 2 illustrates the Tafel curves of the disc samples, where higher E_{corr} and lower I_d represent better corrosion resistance [24]. The highest corrosion potential of about -1.341

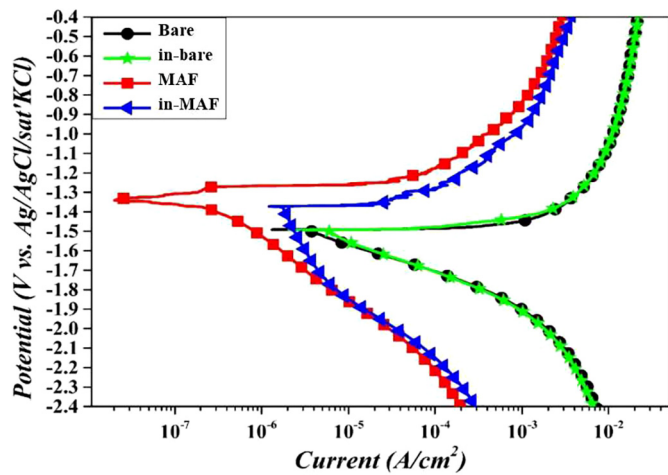


Fig. 2. Potentiodynamic polarization curves of Bare, MAF-coated, indented Bare (in-Bare), and indented MAF-coated (in-MAF) AZ31.

V was obtained from the MAF group, which is higher than the -1.376 V of in-MAF and -1.492 V of Bare and in-Bare. This clearly shows that the MAF coating can significantly improve the corrosion resistance of the magnesium substrate, which is consistent with previous reports [25]. We also found that indentation slightly reduced the corrosion resistance of the MAF coated groups, while the presence of indentation in Bare samples did not have a significant effect. More noteworthy is the MAF group corrosion potential is higher than Bare group (about 0.151 V), there is a potential difference, while exposure will form a primary cell, accelerating the corrosion of the magnesium alloy substrate [26,27].

3.1.2. Immersion tests for indentation sampling system

Fig. 3 shows the optical observations of the in-Bare and in-MAF groups of sampling discs before and after one week of vertical immersion in HBSS solution. The in-Bare group lost the glory and smoothness of the disc surface after one week of immersion, showing superficial and uniform corrosion with no significant enlargement of the indentations. In the in-MAF group, after one week of corrosion, the overall disc did not change significantly and still maintained a good surface gloss and texture. However, when the local dent was amplified, it was found that the indentation was

significantly enlarged and deepened, while expanding in the direction of width and depth, forming a deep pit, in other words, there was a serious fixed-point corrosion. This result is similar to the severe pitting behavior of MAO coating in NaCl solution reported by Yuxiang Liu et al., which means that the indentation is a macroscopic amplification of fixed-point corrosion [17,28]. Fixed-point corrosion accelerates the corrosion of MAF-coated magnesium alloys and reduces the corrosion resistance of the coating itself, while also remarkably affecting the mechanical integrity of the entire sample [16].

In order to first determine whether the coating had been effective in controlling the corrosion rate, the phenomenon of fixed-point corrosion was simulated at the macroscopic level and electrochemical experiments were performed on this system as a priority (Fig. 2). Consistent with previous studies, the data obtained by PDP tests revealed that the prepared coatings were corrosion resistant and notably there was no significant difference between the results of the indent defect group and the others. This means that no clear relationship between the surface defects and the corrosion rate could be extrapolated. On the other hand, after the Hank's Balanced Salt Solution (HBSS) immersion experiments, the defects caused by spot corrosion centered on the dents were clearly observed on the coated samples (Fig. 3). It is nevertheless important that this phenomenon did not eventually appear on the bare Mg samples. The MAF coating has a similar coating structure to the anodized coating while the MAF substrate is more dense [15,25,29,30], thus the condition that a defective/reactive point (e.g., the β phase in Mg alloys) happens to be exposed to the coating through-hole is unlikely possible [31]. However, as the corrosion time increases, the probability of exposure of the defective/active substrate increases with the gradual corrosive process of the surface coating. The indentation of the coating sample is the pitting corrosion source, where the internal Mg substrate is more active and the potential is more negative, while the coating surface potential is more positive (Fig. 2), which may constitute a microcell [27,32]. Furthermore, this area has a large cathode to small anode ratio, which will lead to faster dissolution of the Mg alloy in the pitting source and the formation and gradual enlargement of the etch holes. However, there is no potential difference on the bare Mg alloy sample, so there is no microcell formation, and thus only uniform superficial corrosion occurs.

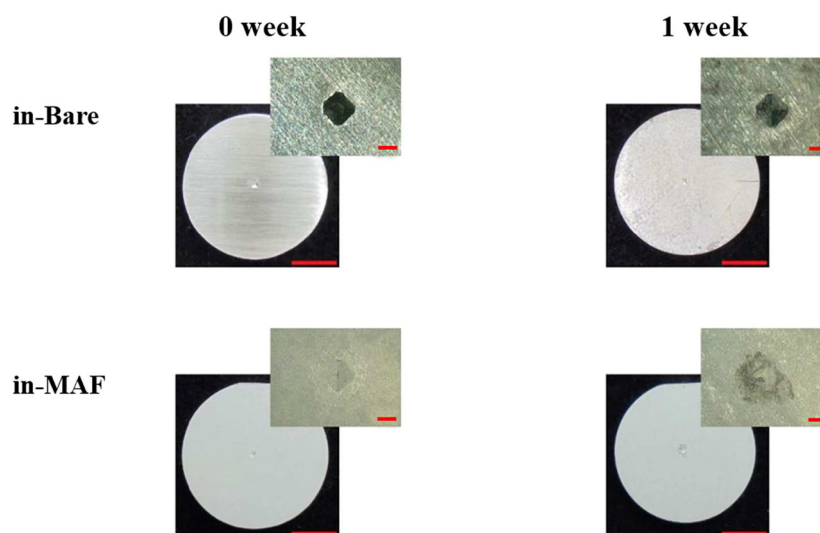


Fig. 3. Optical images of in-Bare group, in-MAF group disc samples before and after one-week test in HBSS. Scale bar of disc optical image, 5 mm; Scale bar of microscopic image at indentation, 500 μ m.

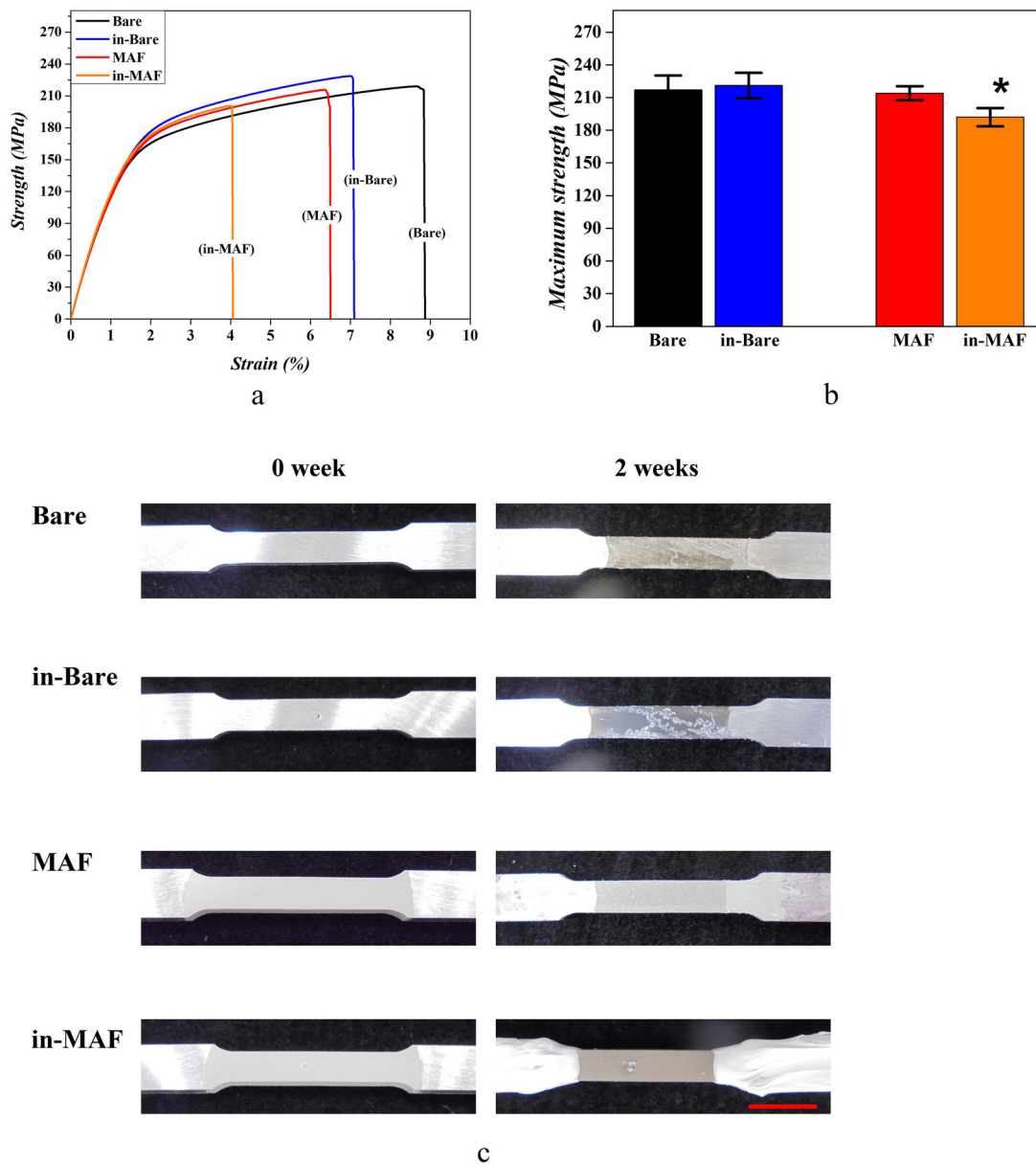


Fig. 4. Mechanical properties of the four sets of samples integrated and optical images of tensile samples before and after two weeks of corrosion. **a**, Typical stress-strain curves. **b**, The mean maximum tensile strength of samples ($n = 10$, $P = 0.05$). **c**, The images show Bare, in-Bare, MAF, and in-MAF tensile samples immersed in simulated body fluids for 2 weeks. Note that the grips on both sides of the tensile samples are sealed with silicon to ensure that they are not involved in degradation and to prevent the clamps from failing during the tensile test due to stress concentration. Scale bar, 10 mm.

3.2. Tensile tests of indentation sampling sets after immersion corrosion

In order to verify that the occurrence of fixed-point corrosion after the surface treatment can significantly affect the mechanical properties of the material, we performed tensile tests after immersion corrosion.

Fig. 4c revealed that the Bare group and in-Bare group samples showed an unsmooth appearance in their respective corrosion areas, showing a large area of corrosion, but no obvious spot corrosion, which can be considered as uniform corrosion to some extent. Moreover, compared with the samples obtained from Fig. 3, the fixed-point corrosion of in-MAF after 2 weeks of immersion is more obvious, indicating that the fixed-point corrosion will continue to spread and deepen with time after appearing [31,32], which is also consistent with the study of J.D. Barajas et al. Scale bar, 10 mm.

Tensile tests were performed on samples after 2 weeks of corrosion in order to verify that fixed-point corrosion in the coating can significantly affect the mechanical properties of the material (Fig. 4a, b). The stress-strain curves and maximum tensile strength were recorded for Bare, in-Bare, MAF, and in-MAF using an INSTRON tester at a constant cross-head speed of 1 mm/min. The curves of each group largely coincided during the elastic deformation phase, indicating that the adhesion of the coating and the dents [33]. However, the tensile strength of the samples decreased in the order of in-Bare > Bare > MAF > in-MAF. Among them, in-Bare has a higher maximum tensile strength, probably due to the protection of its surface corrosion product deposition [34]. And in-MAF shows the lowest ultimate strength. Combined with the appearance of fixed-point corrosion of in-MAF in the optical images (Fig. 3, Fig. 4c), the idea that fixed-point corrosion can significantly affect the mechanical properties of the material can be confirmed [1].

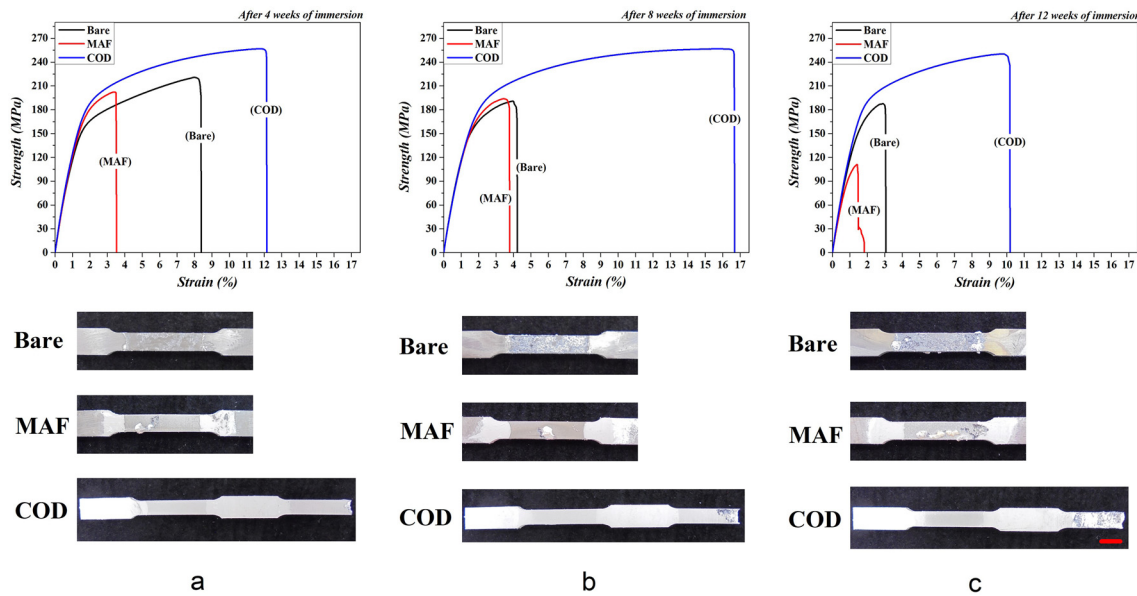


Fig. 5. Stress-strain curves with its optical images of Bare, MAF-coated AZ31, and a COD sample after 4, 8, and 12 weeks of immersion. For maximum tensile strength, **a**, COD > Bare > MAF; **b**, COD > MAF > Bare; **c**, COD > Bare > MAF. With time, the degree of uniform corrosion in the functional area of Bare gradually deepened. Unlike Bare, MAF showed fixed-point corrosion, which appeared only in the central part of the functional area in the first 8 weeks, and gradually extended in the functional area by 12 weeks. (The changes in the Bare and MAF are consistent with Fig. 2, 3.) For the COD, the critical functional area was free of corrosion, while significant corrosion was observed on the surface of leakage in the sacrificial centralized area in the first 4 weeks, and as time went on, the fixed-point corrosion extended from the leaking side to the coating side, which also led to a gradual decrease in the length and thickness of the sacrificial centralized area. Scale bar, 6 mm.

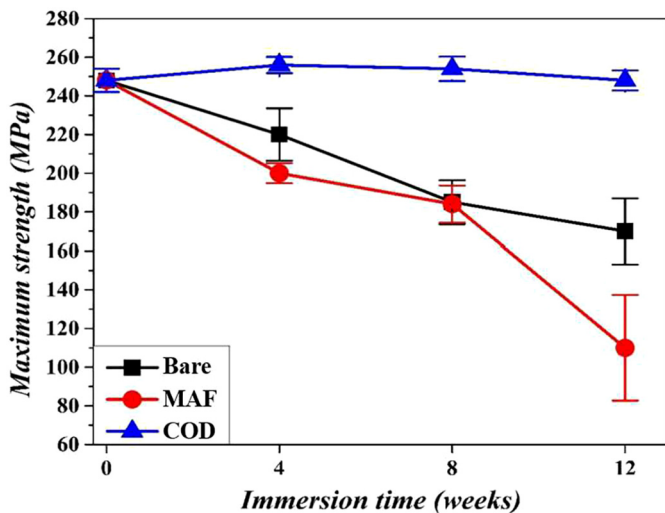


Fig. 6. Mean maximum tensile strength of samples from Bare, MAF, and COD for each specified period of corrosion ($n = 10$, $P = 0.05$). During the 12 weeks of immersion, the tensile strength of COD was always much higher than that of MAF and Bare, while the tensile strength of Bare was all higher or equal to that of MAF. For the COD, there is no significant difference between the non-immersed and the 12-week-immersed. On the contrary, the tensile strength of Bare decreased fast in the first 8 weeks and slower in week 8-12, and decreased to 68.5% of the original strength in week 12. However, the MAF exhibited a different decreasing trend from the Bare, which decreased fast in the first 4 weeks and week 8-12, and slower in week 4-8, decreasing to 44.2% at week 12.

To determine if pitting corrosion on the coated samples was associated with loss of mechanical properties, we next performed sample tensile properties testing (Fig. 4a, b). Stress-strain curves as well as maximum strengths were recorded for the four groups of samples, implying that the presence or absence of indentations did not have a significant impact on the mechanical properties of the homogeneous uncoated samples. Intriguingly, the tensile strength was higher in the indent-treated uncoated group, considering that the specimens were more prone to the deposition of

the corrosion product $Mg(OH)_2$ at the horizontal surface shallow indent, corresponding to a local protective film [17]. Conversely, for coated samples with indentation treatment, more pronounced pitting corrosion can be observed due to the destruction of the coating surface and the exposure of the protected interior, which has a greater weakening effect on the strength of the sample. We believe that the fixed-point corrosion of the coated specimen extends to depth, resulting in a decrease in the actual cross-sectional area of the tensile specimen. In this case, once the same magnitude of stress is applied, the local compressive strength of the material will increase and thus fracture is more likely to occur, in other words, this situation reduces the tensile strength of the material. This enlightens us that the avoidance of fixed-point corrosion becomes an essential role, in order to target the further development of biodegradable Mg alloy materials.

3.3. Assessment of COD models for the control of pitting corrosion phenomena

Mg and Mg alloys exhibit active corrosion performance in HBSS immersion experiments, where the integral corrosion principle can be translated into two partial electrochemical reactions as follows.



By observing each sample after the immersion experiment, it was found that the fixed-point corrosion on the COD samples was confined to the specified area. At the same time, the stress-strain curves showed that the COD sample functional area did not show visible reduction at multiple time points during the immersion period (Fig. 5). A joint analysis of the maximum stress tolerated by all experimental samples and the immersion time shows that the COD samples can maintain excellent mechanical properties for a prolonged period of time (Fig. 6).

4. Discussion

What can also be observed from Fig. 5 is that the length of the corrosion concentration zone in the COD design is decreasing as the corrosion time increases. This is in line with the initially predicted phenomenon of directional corrosion extension, where magnesium-based dissolution starts from the uncoated side and gradually progresses towards the outer coating and the interior. The corrosion condition in the extended section may be worse than in the Bare group, due to the potential difference between the MAF coated AZ31 and the bare AZ31, which may also incur a faster rate of magnesium ion release, hydrogen release and a higher local pH than the bare AZ31 [8,15,30]. However, too high a magnesium ion can incur a high local osmotic pressure [11], which is detrimental to cell proliferation. Secondly, too rapid a rate of hydrogen precipitation ($>0.01 \text{ ml cm}^{-2}/\text{day}$) will also cause problems of tissue separation, necrosis of perioperative tissue, and obstruction of blood flow, although subcutaneous air pockets created by the implantation of the bare AZ31 fracture fixation device into the animal have not disrupted fracture healing or the health of the surrounding tissue after timely removal at some point [8]. The pH range of >7.9 was found to inhibit the osteogenic differentiation of human bone marrow mesenchymal stem cells (hBMSCs), and, more severely, the mineralization of the extracellular matrix was completely inhibited at this pH condition [35]. However, there is no direct data on the overall corrosion rate, hydrogen precipitation rate or pH change of COD in this experiment. This will be the next step in our experimental research.

In previous studies, pitting corrosion has been shown to have a critical effect on the mechanical properties of magnesium alloys through the same corrosion mechanism we mentioned above [36]. It is noteworthy that this phenomenon is more evident at longer corrosion duration [37]. For coated magnesium alloys, pitting corrosion often leads to coating cracking, resulting in its failure, especially for magnesium alloys with a large difference in thermal expansion coefficient between the coating and the substrate [38]. In addition, corrosion-assisted cracking phenomena, such as stress corrosion cracking (SCC) formed by a combination of corrosive environments and mechanical loading, will reduce the mechanical properties of magnesium alloy bone implants more, compared to air corrosion, through pitting corrosion, anodic dissolution, and hydrogen embrittlement (HE) [39,40].

It is widely recognized that in an ideal fracture repair treatment, the implant should be perfectly matched to the injured tissue reconstruction process, meaning that the implant should provide almost nondestructive mechanical support in the early period, while gradually degrading at an acceptable rate in the later stages [41]. The primary purpose of the entire repair process is to circumvent the risk of osteoporosis and other risks that may be associated with the stress shielding effect. More importantly, it is well-established that different bones heal at different rates, which also requires a highly controllable rate of degradation and mechanical properties of the implants. Based on the understanding of the restorative treatment process, we obtain the new design of COD for implants. In the same logic as the dent-treated coated samples, the COD model leaves the uncoated face as the occurrence center of the fixed-point corrosion, where small potential discrepancies may exist at the sample microstructure level. This process may achieve a cathodic protection effect similar to that of sacrificial anodes [42,43], while retaining the coating's role in controlling the corrosion rate of the Mg alloys [32,44]. To a large extent, this avoids stress corrosion cracking and corrosion fatigue caused by fixed-point corrosion [39,45], while simultaneously reducing the risk of secondary trauma caused by Mg alloy materials as implants. Therefore, we hope to use this design to apply to medical magnesium alloy bone plate, expecting this design could ameliorate the

status that existing magnesium alloy bone plate failed to furnish sufficient mechanical support in the pre-bone healing period due to fixed-point corrosion.

It is certain that the corrosion-oriented model we have designed can provide absolute protection over a period of time, but due to the short duration of the experiment, no measurements were made on the exact time. Our next step is to carry out long-term experiments and design our model to meet the time required for bone healing by the length of the corrosion concentration zone, the cross-sectional area, etc. In the conventional sacrificial anode method, anodes of the same weight but different shapes may have different outputs, as the ratio of surface area to weight is not always consistent. Therefore, shape change will play a role when considering current output. Therefore, the shape size of the magnesium alloy in the sacrificial concentration zone for the new COD design in this paper remains to be explored and improved. In addition, we have only conducted *in vitro* experiments, whereas the *in vivo* environment is more complex and subject to a number of factors that may vary the results, so we believe that reasonable *in vivo* experiments are also necessary.

5. Conclusion

1. Electrochemical experiments combined with *in vitro* immersion corrosion tests have demonstrated the corrosion resistance of the multi-prepared magnesium fluoride coating in this study
2. Tensile tests and optical observations on dent-deficient sample lines were used to determine that the phenomenon of fixed-point corrosion is the main cause of the loss of mechanical properties of the material
3. Design of a new model for COD to overcome fixed point corrosion and achieve directional control of the corrosion process in magnesium alloy materials.

This innovative design for Mg alloy materials maintains the excellent mechanical properties of the samples for a long time. Despite the challenging nature of the model, these positive results suggest that this particular tool holds good promise. This may be a step forward for Mg alloy biodegradable materials to achieve clinical repair applications.

Human and animal rights

The authors declare that the work described has not involved experimentation on humans or animals.

Funding

This work did not receive any grant from funding agencies in the public, commercial, or not-for-profit sectors.

Author contributions

All authors attest that they meet the current International Committee of Medical Journal Editors (ICMJE) criteria for Authorship.

CRediT authorship contribution statement

Jian-Hua Zhu: Writing – Original Draft; Validation. **Xinzhe Gao:** Writing – Original Draft; Conceptualization. **Biying Shi:** Writing – Original Draft; Methodology. **Jiawei Zou:** Data analysis. **Yu Ru Li:** Data analysis. **Ke Zeng:** Methodology. **Qi Jia:** Validation. **Heng Bo Jiang:** Writing – Review & Editing; Supervision; Project administration.

Declaration of competing interest

The authors declare that they have no known competing financial or personal relationships that could be viewed as influencing the work reported in this paper.

Data availability

The data used in this paper are available from the corresponding authors upon reasonable request.

References

- [1] Hou R, et al. In vitro evaluation of the ZX11 magnesium alloy as potential bone plate: degradability and mechanical integrity. *Acta Biomater* 2019;97:608–22.
- [2] Hornberger H, Virtanen S, Boccaccini AR. Biomedical coatings on magnesium alloys - a review. *Acta Biomater* 2012;8(7):2442–55.
- [3] Ali M, Hussein MA, Al-Aqeeli N. Magnesium-based composites and alloys for medical applications: a review of mechanical and corrosion properties. *J Alloys Compd* 2019;792:1162–90.
- [4] Rahman M, Li Y, Wen C. HA coating on Mg alloys for biomedical applications: a review. *J Magnes Alloys* 2020;8(3):929–43.
- [5] Wang N, et al. Magnesium alloys for orthopedic applications: a review on the mechanisms driving bone healing. *J Magnes Alloys* 2022;10(12):3327–53.
- [6] Esmaily M, et al. Fundamentals and advances in magnesium alloy corrosion. *Prog Mater Sci* 2017;89:92–193.
- [7] Lotfipour M, et al. In- vitro corrosion behavior of the cast and extruded biodegradable Mg-Zn-Cu alloys in simulated body fluid (SBF). *J Magnes Alloys* 2021;9(6):2078–96.
- [8] Chaya A, et al. In vivo study of magnesium plate and screw degradation and bone fracture healing. *Acta Biomater* 2015;18:262–9.
- [9] Li S, et al. Ultrasonic treatment induced fluoride conversion coating without pores for high corrosion resistance of Mg alloy. *Coatings* 2020;10(10):996.
- [10] Kang MH, et al. MgF₂-coated porous magnesium/alumina scaffolds with improved strength, corrosion resistance, and biological performance for biomedical applications. *Mater Sci Eng C, Mater Biol Appl* 2016;62:634–42.
- [11] Yu W, et al. In vitro and in vivo evaluation of MgF₂ coated AZ31 magnesium alloy porous scaffolds for bone regeneration. *Colloids Surf B, Biointerfaces* 2017;149:330–40.
- [12] Kannan MB, Orr L. In vitro mechanical integrity of hydroxyapatite coated magnesium alloy. *Biomed Mater* 2011;6(4):045003.
- [13] Song R, et al. Effect of corrosion on mechanical behaviors of Mg-Zn-Zr alloy in simulated body fluid. *Front Mater Sci* 2014;8(3):264–70.
- [14] Bobby Kannan M, et al. Hydrogen-induced-cracking in magnesium alloy under cathodic polarization. *Scr Mater* 2007;57(7):579–81.
- [15] Gao X, et al. In vivo corrosion behavior of biodegradable magnesium alloy by MAF treatment. *Scanning* 2021;2021:5530788.
- [16] van Gaalen K, et al. Automated ex-situ detection of pitting corrosion and its effect on the mechanical integrity of rare earth magnesium alloy - WE43. *Bioact Mater* 2022;8:545–58.
- [17] Liu Y, et al. Understanding pitting corrosion behavior of AZ91 alloy and its MAO coating in 3.5% NaCl solution by cyclic potentiodynamic polarization. *J Magnes Alloys* 2021.
- [18] Zhang Z, et al. In-situ monitoring of pitting corrosion of AZ31 magnesium alloy by combining electrochemical noise and acoustic emission techniques. *J Alloys Compd* 2021:878.
- [19] Song Y, et al. Biodegradable behaviors of AZ31 magnesium alloy in simulated body fluid. *Mater Sci Eng C* 2009;29(3):1039–45.
- [20] Simões AM, et al. SVET and SECM imaging of cathodic protection of aluminium by a Mg-rich coating. *Corros Sci* 2007;49(10):3838–49.
- [21] Song G-L, et al. The possibility of forming a sacrificial anode coating for Mg. *Corros Sci* 2014;87:11–4.
- [22] Yu B, Uan J. Sacrificial Mg film anode for cathodic protection of die cast Mg-9wt.%Al-1wt.%Zn alloy in NaCl aqueous solution. *Scr Mater* 2006;54(7):1253–7.
- [23] Yan L, Song G-L, Zheng D. Magnesium alloy anode as a smart corrosivity detector and intelligent sacrificial anode protector for reinforced concrete. *Corros Sci* 2019;155:13–28.
- [24] Hort N, et al. Magnesium alloys as implant materials—principles of property design for Mg-RE alloys. *Acta Biomater* 2010;6(5):1714–25.
- [25] Dai CY, et al. Corrosion evaluation of pure Mg coated by fluorination in 0.1 M fluoride electrolyte. *Scanning* 2021;2021:5574946.
- [26] Liu RL, et al. Controlling the corrosion and cathodic activation of magnesium via microalloying additions of Ge. *Sci Rep* 2016;6:28747.
- [27] Iglesias C, et al. Fracture bone healing and biodegradation of AZ31 implant in rats. *Biomed Mater* 2015;10(2):025008.
- [28] Jia X, et al. Influence of indentation size on the corrosion behaviour of a phosphate conversion coated AZ80 magnesium alloy. *J Mater Res Technol* 2021;14:1739–53.
- [29] Jiang HB, et al. Achieving controllable degradation of a biomedical magnesium alloy by anodizing in molten ammonium bifluoride. *Surf Coat Technol* 2017;313:282–7.
- [30] Jiang HB, et al. Surface modification of anodized Mg in ammonium hydrogen fluoride by various voltages. *Surf Coat Technol* 2014;259:310–7.
- [31] Song G-L, Shi Z. Corrosion mechanism and evaluation of anodized magnesium alloys. *Corros Sci* 2014;85:126–40.
- [32] Barajas JD, et al. Relationship between microstructure and formation-biodegradation mechanism of fluoride conversion coatings synthesised on the AZ31 magnesium alloy. *Surf Coat Technol* 2019;374:424–36.
- [33] Gao H, et al. In vitro and in vivo degradation and mechanical properties of ZEK100 magnesium alloy coated with alginate, chitosan and mechano-growth factor. *Mater Sci Eng C, Mater Biol Appl* 2016;63:450–61.
- [34] Li Z, et al. In vitro and in vivo corrosion, mechanical properties and biocompatibility evaluation of MgF₂-coated Mg-Zn-Zr alloy as cancellous screws. *Mater Sci Eng C, Mater Biol Appl* 2017;75:1268–80.
- [35] Monfoulet LE, et al. The pH in the microenvironment of human mesenchymal stem cells is a critical factor for optimal osteogenesis in tissue-engineered constructs. *Tissue Eng, Part A* 2014;20(13):1827–40.
- [36] AbdelGawad M, et al. Corrosion behavior of Mg-Zn-Zr-RE alloys under physiological environment - impact on mechanical integrity and biocompatibility. *J Magnes Alloys* 2022;10(6):1542–72.
- [37] Adekanmbi I, et al. Mechanical behaviour of biodegradable AZ31 magnesium alloy after long term in vitro degradation. *Mater Sci Eng C, Mater Biol Appl* 2017;77:1135–44.
- [38] Pyun S-I, et al. Relationship between interfacial reaction and adhesion at PVD TiO₂ film-metal (Ti or Al) interfaces. *Surf Coat Technol* 1993;61(1):233–7.
- [39] Peron M, et al. Enhancement of stress corrosion cracking of AZ31 magnesium alloy in simulated body fluid thanks to cryogenic machining. *J Mech Behav Biomed Mater* 2020;101:103429.
- [40] Peron M, et al. Improving stress corrosion cracking behavior of AZ31 alloy with conformal thin titania and zirconia coatings for biomedical applications. *J Mech Behav Biomed Mater* 2020;111:104005.
- [41] Zheng YF, Gu XN, Witte F. Biodegradable metals. *Mater Sci Eng, R Rep* 2014;77:1–34.
- [42] Luba M, et al. Electrochemical degradation of industrial dyes in wastewater through the dissolution of aluminum sacrificial anode of Cu/Al macro-corrosion galvanic cell. *Molecules* 2020;25(18):4108.
- [43] Zeng D, et al. Fracture failure analysis of the sacrificial anode protector in a water injection well. *Eng Fail Anal* 2020;112:104479.
- [44] Javidparvar AA, Naderi R, Ramezanzadeh B. Designing a potent anti-corrosion system based on graphene oxide nanosheets non-covalently modified with cerium/benzimidazole for selective delivery of corrosion inhibitors on steel in NaCl media. *J Mol Liq* 2019;284:415–30.
- [45] Dai H, et al. Pits formation and stress corrosion cracking behavior of Q345R in hydrofluoric acid. *Corros Sci* 2020;166:108443.